


Article

Effects of ZnFe_2O_4 Nanoparticles on Development and Rhythmic Behavior of *Drosophila melanogaster*

Wenhao Yan ¹, Yunfan Guo ¹, Penghui Li ², Ziyang Zhang ², Jinjun Yang ¹  and Yongyan Sun ^{1,*}¹ School of Environmental Science and Safety Engineering, Tianjin University of Technology, Tianjin 300384, China² Institute of Urban Environment, Chinese Academy of Sciences, Xiamen 361021, China

* Correspondence: yongyansun@email.tjut.edu.cn; Tel.: +86-22-60214185

Abstract

Objectives: This study planned to determine the biological effects associated with ZnFe_2O_4 -NPs exposure using *Drosophila melanogaster* as an in vivo model. **Methods:** ZnFe_2O_4 -NPs were hydrothermally synthesized, and the development of offspring flies were evaluated via dietary exposure to different doses of ZnFe_2O_4 -NPs (0, 200, 400, 600 $\mu\text{g/mL}$). Rhythmic behaviors of parent male flies were monitored. **Results:** Internalization of ZnFe_2O_4 -NPs through the intestinal barrier occurred. Oral intake of ZnFe_2O_4 -NPs decreased the eclosed adult numbers and perturbed the insect developmental process. In male flies, significant upregulation of HSPs and Turandot family genes was detected, accompanied by ROS reduction and suppressed antioxidant defense responses, and exposure of ZnFe_2O_4 -NPs disrupted sleep patterns of males, including a reduction in sleep duration and aggravation of sleep fragmentation. Suppressed activity levels were also found after ZnFe_2O_4 -NPs exposure. Significant increased expressions of circadian genes (*Clk* and *Cyc*) were detected, alongside elevation of neurotransmitter levels and related gene expressions. **Conclusions:** Overall, ZnFe_2O_4 -NPs can perturb development process via inducing heat shock and detoxification response, and disrupted rhythmic behaviors may be attributed to elevation of neurotransmitter levels and upregulated gene expressions of circadian genes. Our findings may offer valuable insights for evaluating ecological risks of metal-based nanoparticles and suggest potential applications in developing novel pest management strategies by utilizing insect behavioral and physiological responses to nanomaterials.

Keywords: *Drosophila melanogaster*; ZnFe_2O_4 -NPs; rhythmic behavior; development; stress responses



Academic Editors: Yankai Xia, Ruijia Zhang and Jamie L. Inman

Received: 17 August 2025

Revised: 7 September 2025

Accepted: 10 September 2025

Published: 14 September 2025

Citation: Yan, W.; Guo, Y.; Li, P.; Zhang, Z.; Yang, J.; Sun, Y. Effects of ZnFe_2O_4 Nanoparticles on Development and Rhythmic Behavior of *Drosophila melanogaster*. *Toxics* **2025**, *13*, 779. <https://doi.org/10.3390/toxics13090779>

Copyright: © 2025 by the authors. Licensee MDPI, Basel, Switzerland. This article is an open access article distributed under the terms and conditions of the Creative Commons Attribution (CC BY) license (<https://creativecommons.org/licenses/by/4.0/>).

1. Introduction

With the rapid advancement of nanotechnology in recent decades, utilization of magnetic nanoparticles has been significantly accelerated, leading to their integration into a wide range of fields. Magnetic nanoparticles have been widely applied in various fields, including drug delivery, medical imaging, biosensing, and photocatalysis [1–4]. Among the magnetic nanoparticles, ferrite particles have garnered particular attention due to their excellent biocompatibility, tunable magnetic properties, and ease of synthesis [5,6]. These characteristics make them ideal candidates for a wide range of applications, including magnetic resonance imaging (MRI), magnetic hyperthermia, and environmental remediation. Ferrite nanoparticles (MFe_2O_4) were usually synthesized through metal doping (where M = Fe^{2+} , Mg^{2+} , Co^{2+} , Ni^{2+} , Zn^{2+} , Mn^{2+} , etc.) [7]. In recent years, the zinc ferrite

nanoparticles (ZnFe₂O₄-NPs) market has seen significant growth, propelled by advancements in nanotechnology and increased adoption in sectors such as healthcare, electronics, and environmental remediation [8]. Ferrite market size was valued at USD 5 billion in 2023 and forecast to reach around USD 6.38 billion by 2030. Zinc ferrite nanoparticles account for about 5% of the ferrite market scale, and it is expected that the annual average production will reach 375 tons by 2030 [9]. Assuming that the release rate in the industrial production process is 0.1–1% (referring to the average release factor of the nanomaterial industry [10]), tons of zinc ferrite nanoparticles may enter the environment every year. Zinc ferrite nanoparticles of around 100 nm can be used not only in photodynamic therapy but also for gas monitoring in the environment [11,12]. Studies have focused on the environmental transport, transformation, and toxicity of engineered nanomaterials such as iron oxides, zinc oxide, silver nanoparticles, and titanium dioxide. These studies have confirmed that these nanomaterials are released into environmental media including soil, water, and air, and trigger related ecological risks [13,14]. Currently, there are no established release standards or regulations for magnetic nanoparticles, raising concerns about their potential adverse effects on living organisms. The potential for magnetic nanoparticle release to environment was expected to increase, while the environmental and ecological risks caused by ZnFe₂O₄-NPs release remain unclear.

Recent studies revealed various biological responses to different ferrite nanoparticles. For example, silver ferrite nanoparticles were shown to extend the lifespan of female *Drosophila melanogaster* (*D. melanogaster*) and enhance offspring production [15]. Iron accumulation and toxicity were induced via iron oxide nanoparticles oral intake in *D. melanogaster*, accompanied by weakened female reproductive capacity and delayed developmental transition. A concentration of 1000 mg/kg Fe₃O₄-NPs reduced the number of offspring in *Drosophila* [16]. Wing deformities were induced under iron oxide nanoparticle exposure [17], and an 80 µg/mL Fe₃O₄ nanocomposite decreased the crawling speed of *Drosophila* larvae and the body weight of adult *Drosophila* [18]. In zebrafish, iron oxide nanoparticles can induce circadian dysregulation, characterized by elevating average activity speed and reducing sleep frequency [19]. Fe₃O₄-NPs enhanced photosynthetic pigment content, biomass, and stress resilience in wheat (especially under salinity) and tomato [20]. These findings collectively suggested that upon entering the ecological environment, various ferrite nanomaterials can induce multiple effects on the development, and behavior of both animals and plants. A previous study has found that 200 µM of ZnFe₂O₄@poly(tBGE-alt-PA) nanocomposite caused weakened climbing ability, decreased body weight, and broken wing venation in adult flies [21]. Although the applications and releases into the environment are increasingly growing, the mechanisms and bioeffects of ZnFe₂O₄-NPs in living organisms remain insufficiently studied.

In this study, *D. melanogaster* was selected as an experimental model not only due to its well-characterized genetic background and short life cycle, but also for its distinct advantages in nanotoxicology research [22]. As a terrestrial organism, it provides relevant insights into nanoparticle exposure through land ecosystems [23]. Its genetic tractability enables precise investigation of nanoparticle uptake and toxicity mechanisms [24]. For example, the dietary intake of AgNPs in the early larval stage led to behavioral abnormalities in *D. melanogaster*, such as poorer crawling and climbing abilities in larvae and adults [25]. Flawed climbing behavior against gravity was seen in ZrO₂ NP-treated flies [26]. Furthermore, due to sleep architecture of *D. melanogaster* shares fundamental with mammals, the advantages of this model organism have also been essential for understanding the molecular nature of circadian (24 h) rhythms and continue to be valuable in discovering novel regulators of circadian rhythms and sleep. Previous studies have found that metal materials can alter the rhythmic behavior of *D. melanogaster*, affecting activity and sleep.

Circadian disruption and sleep disorders are strongly connected to neurodegenerative diseases including Parkinson's disease, Alzheimer's disease, and Huntington's disease as well as others. Metal exposures have been implicated in neurodegenerative diseases, in some cases involving metals that are essential micronutrients but are toxic at high levels of exposure. For example, daily rhythm of activity was disrupted in aged flies under aluminum exposure [27]. These findings collectively suggested that ZnFe₂O₄-NPs may probably affect rhythmic behavior of *D. melanogaster*.

In this study, ZnFe₂O₄-NPs were hydrothermally synthesized and characterized and oral exposure to ZnFe₂O₄-NPs were performed in *D. melanogaster* at concentrations of 0, 200, 400, or 600 µg/mL. Intestinal barrier of parental flies (including male and female) was observed by TEM analysis. Developmental parameters of the offspring were systematically quantified, and rhythmic activity levels and sleep patterns of parent flies were monitored. Simultaneously, mechanisms of ZnFe₂O₄-NPs exposure on *D. melanogaster* were elucidated. This integrated study may highlight the urgent need to investigate the mechanisms of environmental release of ferrite nanoparticles and enrich comprehensive understandings about effects of ferrite nanoparticles on development and rhythmic behaviors in insect populations.

2. Materials and Methods

2.1. Synthesis of ZnFe₂O₄-NPs

ZnFe₂O₄-NPs were synthesized using the hydrothermal method. A mixture of 1.983 mmol of FeCl₃·6H₂O, 0.992 mmol of ZnCl₂, 8.925 mmol of polyvinylpyrrolidone (PVP, K = 30), and 29.75 mmol of CH₃COONa was combined in 35 mL of ethylene glycol and stirred magnetically for 4 h to ensure complete dissolution of the components. All these chemicals were obtained from Sinopharm Chemical Reagent Co., Ltd., Shanghai, China. Subsequently, the solution was transferred to a 50 mL Teflon-lined autoclave (Zhengzhou Keda Machinery Company, Zhengzhou, China), heated to 180 °C for 1 h, and then heated to 200 °C for 8 h. The resulting mixture was washed with deionized water and ethanol (Analytical Reagent, Sinopharm Chemical Reagent Co., Ltd., Shanghai, China). Finally, the sample was vacuum-dried at 40 °C for 12 h to obtain the ZnFe₂O₄-NPs. The residual pressure during vacuum drying was maintained below 133 Pa.

2.2. Characterization of ZnFe₂O₄-NPs

The microstructure of the prepared ZnFe₂O₄-NPs sample was characterized by using SEM (Verios 460L scanning electron microscope, FEI Corporation, Hillsboro, OR, USA). Crystal structure was analyzed via using X-ray diffractometer analysis (XRD, SmartLab 9KW, Rigaku Corporation, Tokyo, Japan). Chemical bonding state of ZnFe₂O₄-NPs was examined by X-ray photoelectron spectroscopy (XPS, Escalab 250Xi system, Thermo Scientific, Waltham, MA, USA).

2.3. Exposure to ZnFe₂O₄-NPs and Experimental Conditions

In this study, the wild-type *D. melanogaster* (W1118) was utilized (Core Facility of Drosophila Resource and Technology, CEMCS, CAS). The ZnFe₂O₄-NPs were thoroughly mixed with the yeast cornmeal standard medium [28] to achieve final concentrations of 200 µg/mL, 400 µg/mL, and 600 µg/mL. These concentrations were determined based on the method described by Chen et al. [29]: using twice the clinical dose of Feridex as the reference. Feridex has a recommended human dose of 0.56 mg Fe/kg body weight [30], and dosage conversion was performed via the body surface area (BSA) ratio between *Drosophila* ($8.8 \times 10^{-6} \text{ m}^2$) and humans (1.71 m^2), yielding an equivalent iron dose of $3.46 \times 10^{-4} \text{ mg}$ per *Drosophila*. Calculations further showed the total ZnFe₂O₄ requirement

for 40 parental flies and 100 offspring was 0.528 mg. Correspondingly, the theoretical concentration for a single administration in *Drosophila* was approximately 200 µg/mL, while for daily administration it was approximately 600 µg/mL. Flies of the control groups were maintained on the same standard medium containing inactivated yeast, sucrose, agar, corn meal, and maltose (all the medium chemicals obtained from Sinopharm Chemical Reagent Co. Ltd., Shanghai, China). All the flies were cultivated in an artificial climate incubator (PQX-450A-3HM, Ningbo Laifu Technology, Ningbo, China) with 25 ± 1 °C, $60 \pm 2\%$ relative humidity, and 12 h light/dark cycle (lights on at 6:00 AM and off at 6:00 PM).

2.4. TEM Analysis of Guts of *D. melanogaster*

To detect the presence of ZnFe₂O₄-NPs in the intestines of the *D. melanogaster*, both male and female parental flies were collected, respectively, and dissected after 72 h exposure to ZnFe₂O₄-NPs. The guts were extracted as previously described [31]. Briefly, parental flies were cleaned and dissected in phosphate buffer (PB; 0.1 M, pH 7.4) and fixed for 2 h in a solution containing 4% paraformaldehyde and 1% glutaraldehyde in 0.15 M phosphate buffer (pH 7.4). Gut tissues were post-fixed for 2 h with 1% (*w/v*) osmium tetroxide containing 0.8% (*w/v*) potassium hexacyanoferrate (prepared in PB), followed by four washes with deionized water and sequential dehydration in acetone. Finally, samples were embedded in Eponate 12TM resin (Ted Pella Inc., Redding, CA, USA) and polymerized at 60 °C for 48 h. Semi-thin sections (1 µm thick) were obtained and stained with 1% (*w/v*) aqueous toluidine blue, and then placed on noncoated 200 mesh copper grids, and contrasted with conventional uranyl acetate (30 min) and Reynolds lead citrate (5 min) solutions (All the chemicals mentioned were obtained from Sigma-Aldrich Technology, St. Louis, MO, USA). Sections of samples were observed with a LaB6 Transmission electron microscopy (100 kV TEM, FEI Company, Hillsboro, OR, USA).

2.5. Developmental Detection Experiments

For each experimental group (0, 200, 400, or 600 µg/mL ZnFe₂O₄-NPs), three replicate culture tubes were prepared, and 20 virgin male–female pairs were collected and placed into each tube. Parental flies were removed after 72 h of oviposition, and cultures were maintained until eclosion of the final offspring (F1 generation). The specific statistical methods about F1 generation were as follows:

Number of pupae: the total number of pupae per tube was counted, with counts commencing upon the emergence of the first pupa and continuing until pupation ceased.

Number of eclosed adults: the cumulative total number of adult *Drosophila* eclosing per tube was recorded from the emergence of the first adult until no further eclosion occurred.

Total offspring count: the sum of the number of pupae and the number of eclosed adults per tube.

Sex ratio: the numbers of male and female *Drosophila* in each tube were recorded separately. The sex ratio was calculated as the number of females divided by the number of males.

Pupation percentages in the first 3 days: the day of the first pupal emergence was designated as day one. The proportion of total pupae formed within the first 3 days was calculated.

Body weight: the weight of each individual eclosed adults (24 h post-eclosion) per tube was determined.

2.6. Monitoring of Rhythmic Behavior in *Drosophila*

Male adults of the F1 generation, collected at 24 h post-eclosion, were used for the behavioral analysis. This experiment followed the established methodology for sleep and

rhythm parameter quantification described by Wang et al. [32]. For each concentration group, 96 flies were individually loaded into tubes (inner diameter: 5 mm; length: 65 mm) of the Drosophila Activity Monitor (DAM2) system (TriKinetics, Waltham, MA, USA). Each tube contained a culture medium (5% sucrose/2% agar, chemicals obtained from Sinopharm Chemical Reagent Co., Ltd., Shanghai, China) supplemented with the corresponding concentration of ZnFe₂O₄-NPs, and flies were maintained under 12 h:12 h light/dark (LD) conditions throughout the experiment. The DAM2 system recorded the activity of each fly every 5 min for a continuous period of at least 3 days. Sleep was defined as a period of continuous immobility lasting ≥ 5 min [33]. The differences in the number of activities (activity counts), unit activity capacity (total activity counts/awake time), sleep duration, number of sleep episodes, mean sleep duration per episode, and activity and sleep rhythms were analyzed. Each experiment was repeated three times.

2.7. Oxidative Stress Analysis and Neurotransmitter Levels Detection

The F1 generation in each group were collected after 24 h post-eclosion, quick-frozen with liquid nitrogen, and stored at -80°C for follow-up detection. Reactive oxygen species (ROS) levels, total antioxidant capacity (T-AOC), superoxide dismutase (SOD) activity (WST-1 method), catalase (CAT) activity (ammonium nitrite method), malondialdehyde (MDA) content, gamma aminobutyric acid (GABA) concentration, and acetylcholine (ACh) levels were measured using specific commercial assay kits (Nan Jing Jian Cheng Bio Inst, Nanjing, China), strictly following the manufacturers' protocols. Integrated optical density (IOD) of Dichlorofluorescein (DCF) were utilized to measure the ROS levels. This method is based on the redox-sensitive fluorescent probe DCFH-DA (2',7'-Dichlorodihydrofluorescein diacetate), and the detection was performed according to standard protocol of the assay kit. Total protein (TP) concentration was quantified using a Total Protein Assay Kit (Kemas Brilliant Blue method; Nan Jing Jian Cheng Bio Inst, Nanjing, China). All assays were performed in triplicate.

2.8. QRT-PCR Detection

The eclosed F1 adults were collected according to the exposure concentration and sex; 30 male and 30 female flies of each concentration were selected for RNA extraction. Total RNA was extracted by TRIzol reagent (Sigma-Aldrich Technology, St. Louis, MO, USA) and reverse transcribed by the Prime Script RT Master Mix Perfect Real Time kit (Takara, Kyoto, Japan), and the Green Premix Ex TaqII kit (Takara, Kyoto, Japan) was used for real-time fluorescence quantitative PCR experiments. The relative expression levels of heat stress family genes (*Hsp26*, *Hsp70*), immune system-related genes (*TotA*, *TotC*), circadian clock genes (*Cyc*, *Clk*), and neurotransmitter-related genes (*Dα1*, *Dβ1*, *ChAT*, *Gat*, *Gad1*) were detected. All samples were tested three times, and the CT values of the target genes were normalized to the CT values of the reference gene *rp49*. The relative quantitative analysis was carried out by the $2^{-\Delta\Delta\text{CT}}$ method [34]. The primers used are shown in Supplementary Table S1.

2.9. Statistical Analysis

The experimental data were analyzed using SPSS 20 (IBM Corporation, Armonk, NY, USA) and Origin 2021 (OriginLab Corporation, North Andover, MA, USA). Differences between the control and exposure groups were analyzed by one-way ANOVA, and LSD method was employed to assess significance. Data were presented as mean \pm SEM of three independent biological replicates. Statistical results are expressed as the mean \pm SEM, $p < 0.05$ represents a statistically significant difference (* $p < 0.05$; ** $p < 0.01$).

3. Results

3.1. SEM Analysis of Nano ZnFe_2O_4 and the TEM Analysis of Intestines of *Drosophila melanogaster*

Morphological analysis by SEM revealed monodisperse spherical particles with an average diameter of approximately 100 nm (Figure 1a). The particle size distribution was further quantified showing a measured value of 164.0 d.nm (Figure 1b). The diffraction peaks observed at 2θ angles of 29.9° , 35.3° , 42.9° , 53.2° , 56.7° , and 62.2° were indexed to the planes (220), (311), (400), (422), (511), and (440), respectively (Figure 1c). The pattern was consistent with the ZnFe_2O_4 -NPs spinel structure as per PDF card # 79-1150. Additionally, the XPS spectra of Fe(2p) and Zn(2p) were detected. The peaks at 711.7 eV (Fe $2p_{3/2}$) and 725.4 eV (Fe $2p_{1/2}$) confirmed Fe^{3+} in the crystal structure, and peaks at 1021.51 eV (Zn $2p_{3/2}$) and 1044.66 eV (Zn $2p_{1/2}$) indicated the Zn^{2+} state in the spinel structure (Figure 1d,e). TEM analysis demonstrated that internalization of ZnFe_2O_4 -NPs through the flies' intestinal barrier was observed (Figure 1f,g).

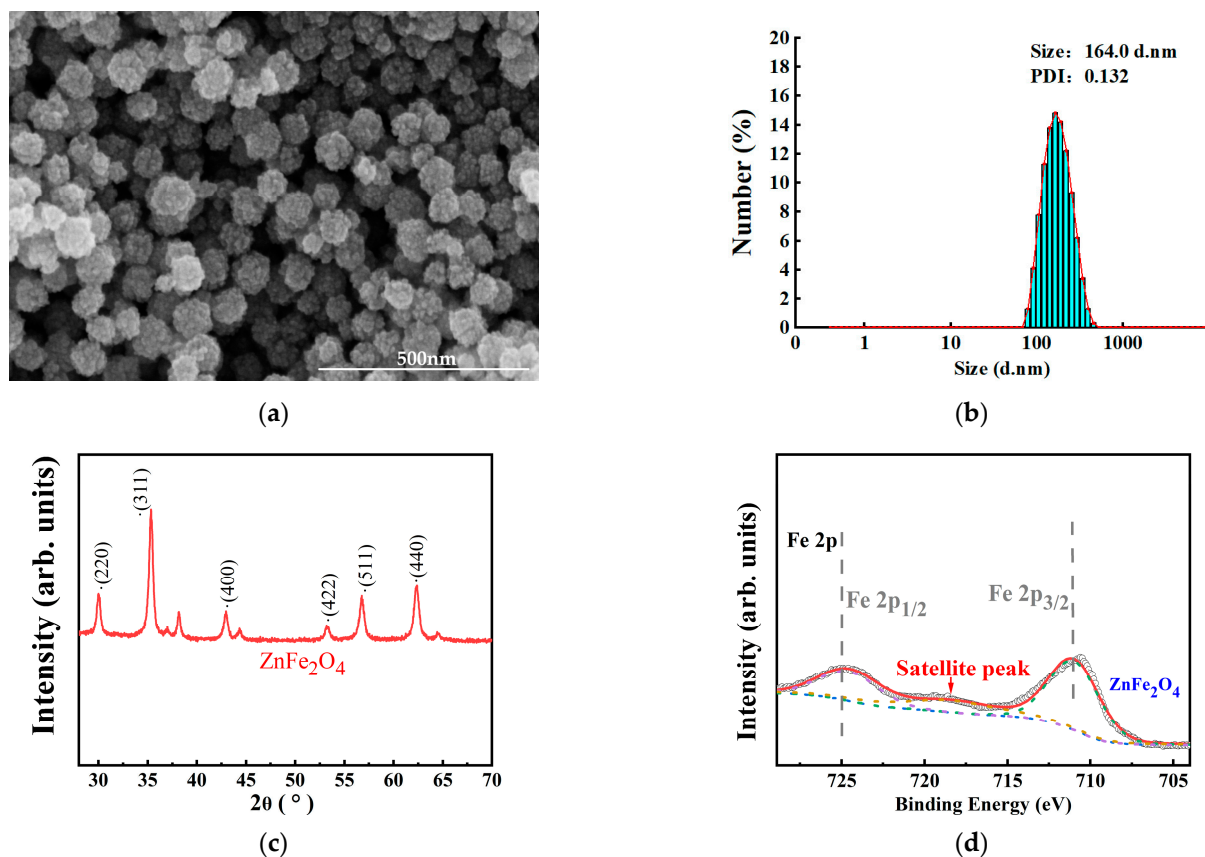
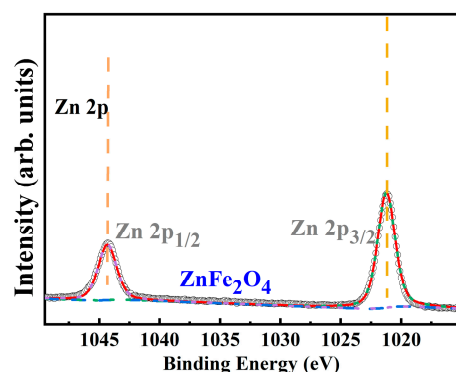
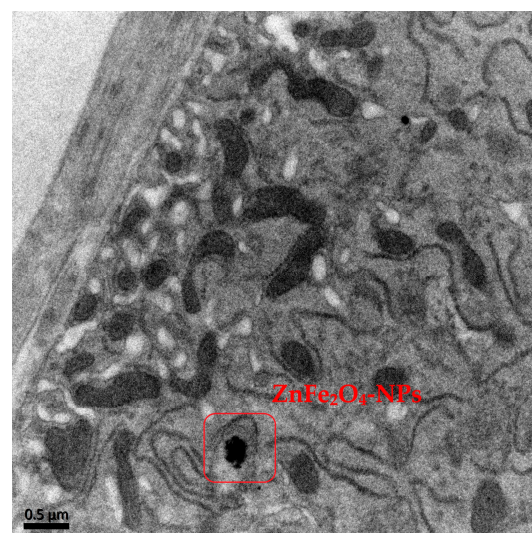


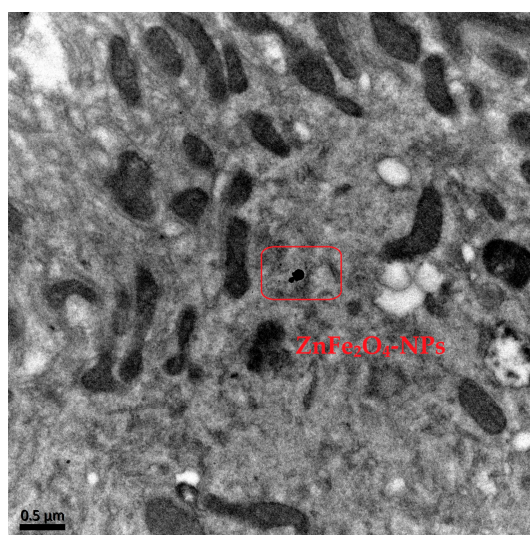
Figure 1. Cont.



(e)



(f)



(g)

Figure 1. (a) The SEM image of ZnFe_2O_4 -NPs. (b) Size distribution of ZnFe_2O_4 -NPs. (c) XRD spectrum of ZnFe_2O_4 -NPs. (d) Fe 2p XPS spectra of ZnFe_2O_4 -NPs. Scatter points represented the experimental data. The red, blue, green, purple, and brown lines corresponded to the overall sum fit, background, Fe^{3+} $2p_{3/2}$ peak, Fe^{3+} $2p_{1/2}$ peak, and satellite peak. (e) Zn 2p XPS spectra of ZnFe_2O_4 -NPs. Scatter points represented the experimental data. The red, blue, green, and purple lines corresponded to the overall sum fit, background, Zn^{2+} $2p_{3/2}$ peak, and Zn^{2+} $2p_{1/2}$ peak. (f) The gut image of the female. (g) The gut image of the male.

3.2. Effects of ZnFe_2O_4 -NPs on Development

After 3 days of exposure, the parental flies were removed from mating vials and the number of offspring surviving to pupal and adult life-stages was counted. Analysis of total offspring production revealed that ZnFe_2O_4 -NPs exposure can significantly increase numbers of offspring, with the most pronounced effects observed at higher concentrations (Figure 2a–c). Total pupation counts were elevated by 32% and 73% after 400 $\mu\text{g}/\text{mL}$ and 600 $\mu\text{g}/\text{mL}$ ZnFe_2O_4 -NPs exposure, respectively (** $p < 0.01$, Figure 2a). Under 200 $\mu\text{g}/\text{mL}$ ZnFe_2O_4 -NPs exposure, pupation rates within the first 3 days were accelerated by 141% (* $p < 0.05$, Figure 2c). For eclosion development, 600 $\mu\text{g}/\text{mL}$ ZnFe_2O_4 -NPs exposure induced a 16% reduction in the number of eclosed adults (* $p < 0.05$, Figure 2b). No

significant differences in female-to-male ratio or body weight of offspring were observed under ZnFe_2O_4 -NPs exposure (Figure 2e,f).

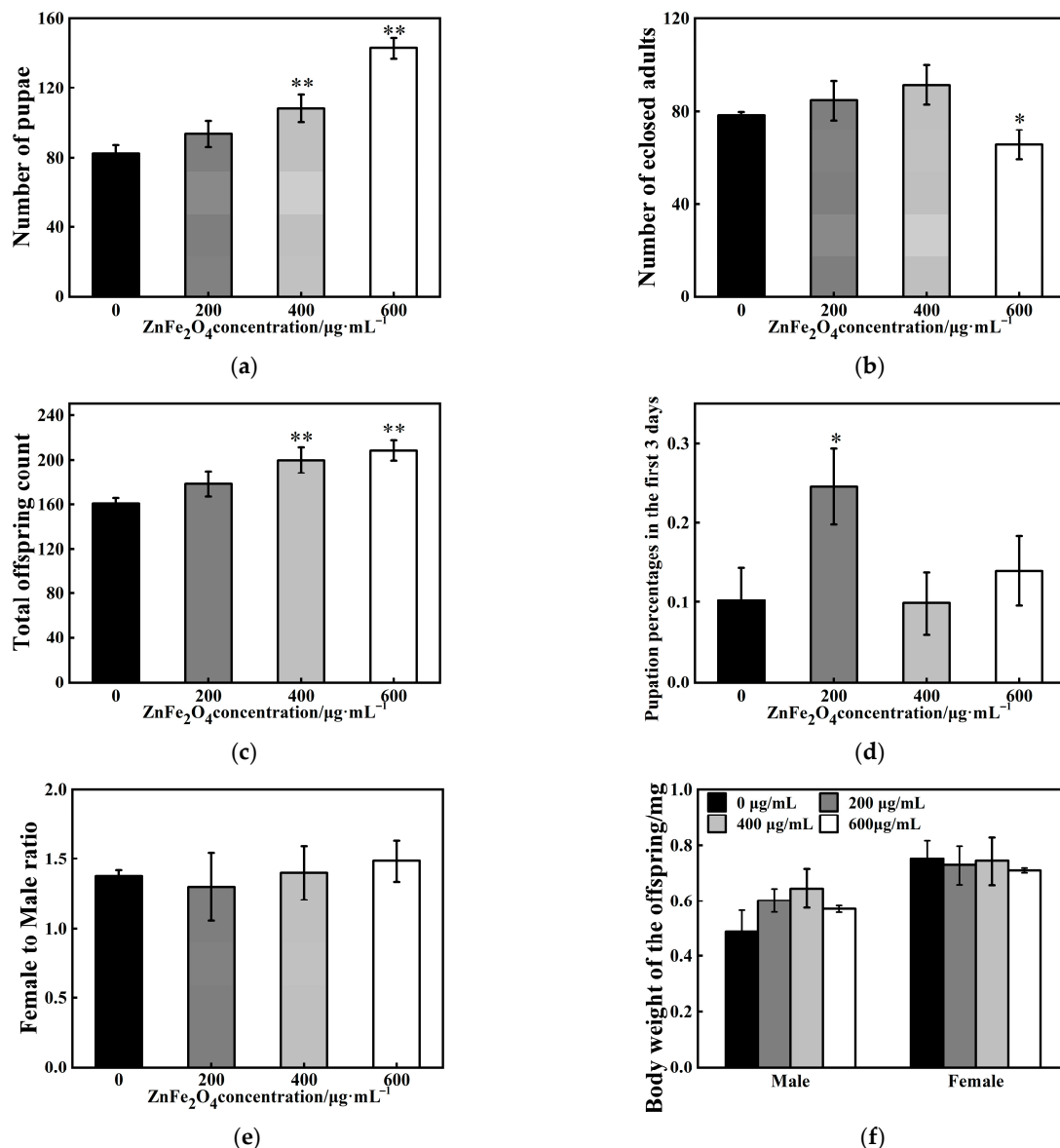


Figure 2. (a) Number of pupae. (b) Number of eclosed adults. (c) Total offspring count. (d) Pupation percentages in the first three days (calculated as: number of pupae formed in first 3 days/total pupae count; value of 0.1 indicates 10% of total pupation occurred in the first three days in control group). (e) Female to male ratio. (f) body weight of the offspring. Values represent mean \pm SEM. (* $p < 0.05$; ** $p < 0.01$).

3.3. Effects of ZnFe_2O_4 -NPs Exposure on Rhythmic Behaviors

The activity results showed that for male flies after ZnFe_2O_4 -NPs exposure, decreased unit activity capacity was observed while there were no statistically significant changes in the number of activities (Figure 3a,b). High concentrations of ZnFe_2O_4 -NPs may induce less unit activity times. The 400 $\mu\text{g}/\text{mL}$ ZnFe_2O_4 -NPs group exhibited 6% decreases in unit activity capacity in 24 h, and the 600 $\mu\text{g}/\text{mL}$ ZnFe_2O_4 -NPs group exhibited 12% and 10% decreases in unit activity capacity in night and 24 h, respectively (* $p < 0.05$, ** $p < 0.01$, Figure 3b). For sleep patterns, decreased sleep duration (5%, ** $p < 0.01$), increased number of sleep episodes (13%, * $p < 0.01$), and decreased mean sleep duration per episode (20%, ** $p < 0.01$) were found under 600 $\mu\text{g}/\text{mL}$ ZnFe_2O_4 -NPs exposure (Figure 3c–e). In addition,

no significant changes were observed except a 15% reduction in mean sleep duration per episode under 400 $\mu\text{g/mL}$ ZnFe_2O_4 -NPs exposure (Figure 3e, * $p < 0.05$). Three-day recording data showed that the exposure groups exhibited similar activity and sleep rhythms as the control groups (0 $\mu\text{g/mL}$), regardless of concentrations of ZnFe_2O_4 -NPs (Figure 3f,g), with an activity peak and a sleep trough at ~6:00 and 18:00, the same as the set light/dark cycles (12 h/12 h, light-on time set at 6:00 AM every day, GMT + 6:00).

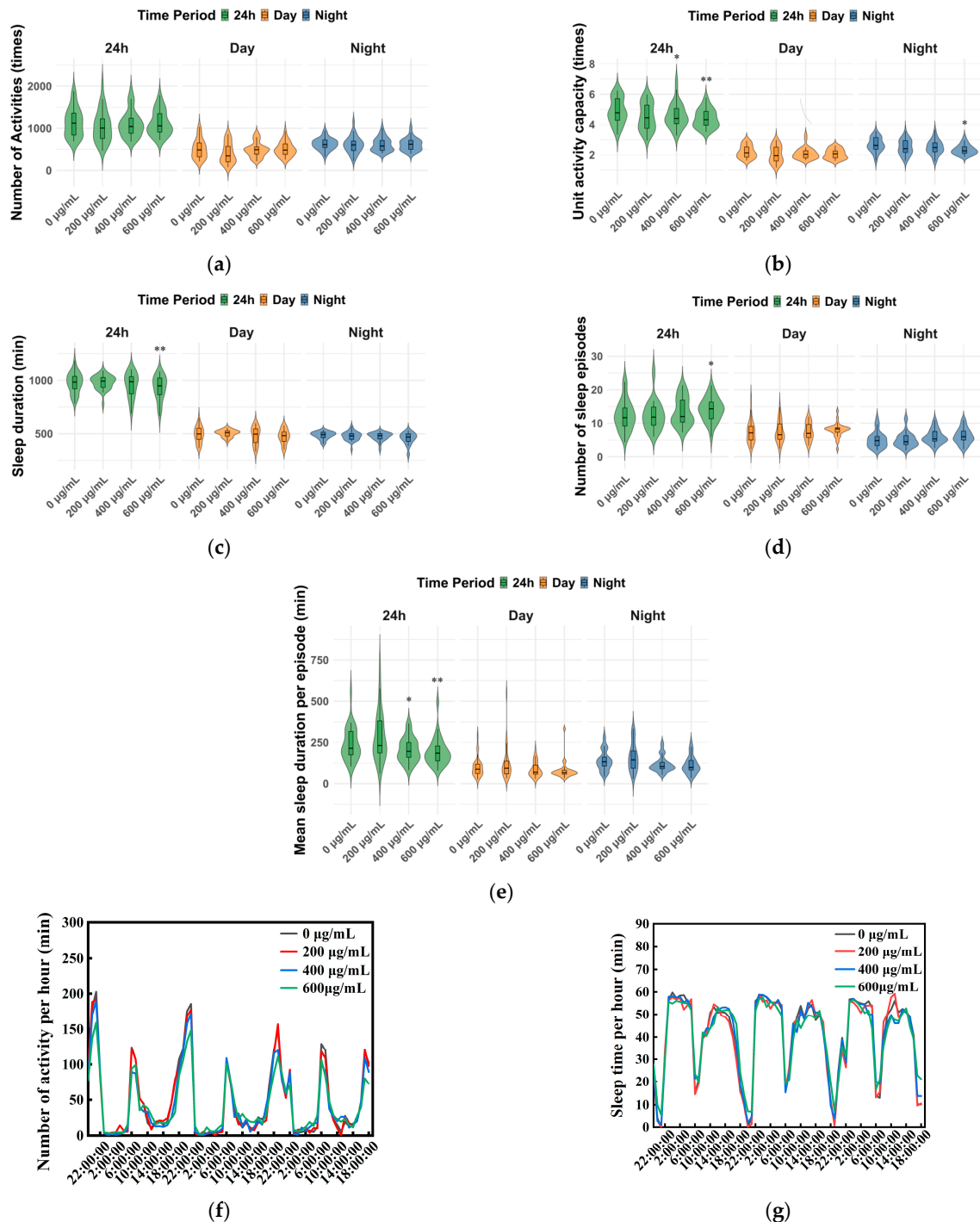


Figure 3. Activity and sleep of male flies under ZnFe_2O_4 -NPs exposure. (a) Number of activities (times). (b) Unit activity capacity (times). (c) Sleep duration (min). (d) Number of sleep episodes. (e) Mean sleep duration per episode (min). (f) Activity pattern diagram in 24 h. (g) Sleep pattern diagram in 24 h. All values are expressed as the means \pm SEM. (* $p < 0.05$; ** $p < 0.01$). At least 90 flies were analyzed in each group.

3.4. Oxidative Stress Responses Under ZnFe_2O_4 -NPs Exposure

The offspring flies were selected and examined after 24 h post-eclosion. The effects of ZnFe_2O_4 -NPs on oxidative stress responses differ between sexes. ROS levels in vivo decreased by 36% in male flies after 600 $\mu\text{g}/\text{mL}$ ZnFe_2O_4 -NPs exposure, while 16% and 29% reduction in ROS contents in females were found, respectively, after 400 $\mu\text{g}/\text{mL}$ and 600 $\mu\text{g}/\text{mL}$ ZnFe_2O_4 -NPs exposure (* $p < 0.05$, ** $p < 0.01$, Figure 4a). For determination of the antioxidant system, T-AOC suppression was found in males flies (11% and 19% under 400 and 600 $\mu\text{g}/\text{mL}$ ZnFe_2O_4 -NPs exposure, respectively), but no significant changes were observed in female flies (Figure 4b). Specifically, ZnFe_2O_4 -NPs weakened the CAT and SOD enzyme activities of male flies, accompanied with depressed MDA levels (* $p < 0.05$, ** $p < 0.01$, Figure 4c–e). Concurrently, the female flies exhibited upregulated CAT and SOD enzyme activities under ZnFe_2O_4 -NPs exposure, accompanied with the reduction in MDA contents (* $p < 0.05$, ** $p < 0.01$, Figure 4c–e).

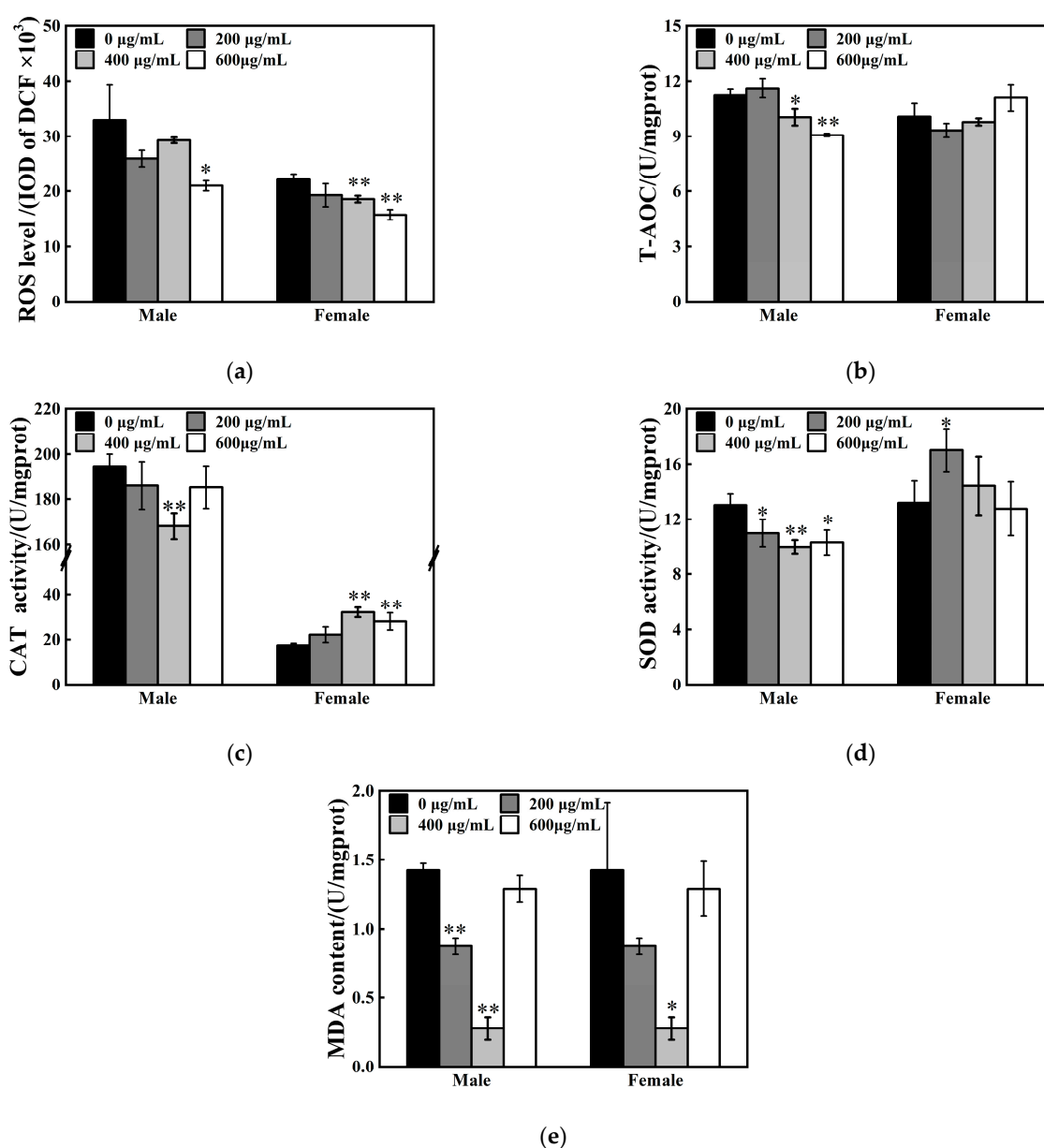


Figure 4. Effects of ZnFe_2O_4 on oxidative stress in flies. (a) ROS levels (Integrated Optical Density of DCF). (b) T-AOC levels. (c) CAT activities. (d) SOD activities. (e) MDA contents. Values represent mean \pm SEM. (* $p < 0.05$; ** $p < 0.01$).

3.5. Effects of ZnFe₂O₄-NPs on Neurotransmitters Levels

To investigate the mechanisms of rhythmic alterations, we examined the neurotransmitter levels in vivo of F1 male flies after ZnFe₂O₄-NPs exposure. The results showed that ACh contents were elevated by 147% and 77% under 400 and 600 µg/mL exposure, respectively (** $p < 0.01$, Figure 5a). In parallel, the 600 µg/mL dose exposure induced a 68% upregulation of GABA (** $p < 0.01$, Figure 5b).

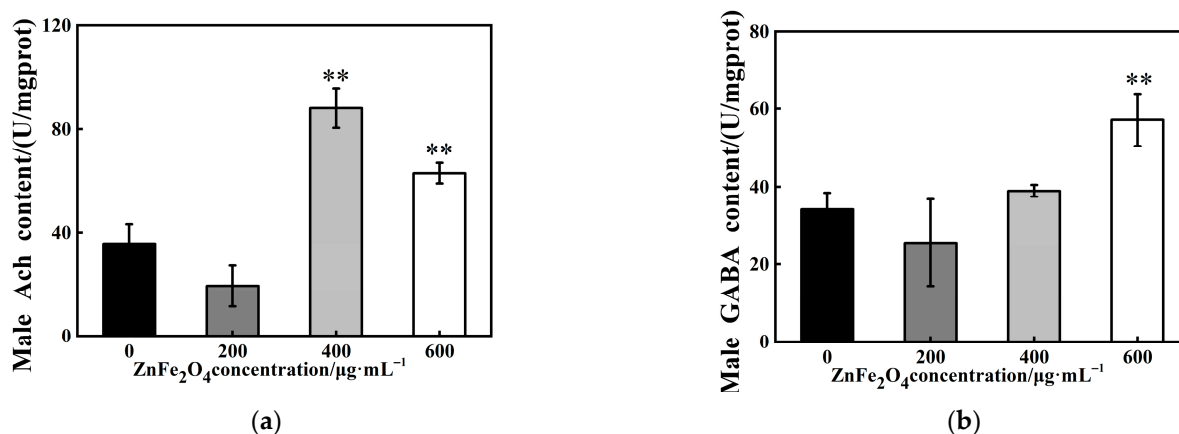


Figure 5. Effects of ZnFe₂O₄-NPs on neurotransmitters levels. (a) ACh content. (b) GABA content. Values represent mean ± SEM. (** $p < 0.01$).

3.6. Relative Expression Levels of Target Genes After ZnFe₂O₄-NPs Exposure

To further elucidate the mechanisms of ZnFe₂O₄-NPs exposure in insects, relative expression levels of heat shock protein encoding genes (*Hsp70*, *Hsp26*) and Turandot family genes (*TotA*, *TotC*) were investigated. *TotA* is a stress-responsive peptide coordinating trade-offs between immunity and reproduction, while *TotC* can mediate metabolic adaptation to nutrient deprivation in *D. melanogaster* [35,36]. In F1 males, significant upregulated relative expression levels of *Hsp70*, *Hsp26*, *TotA* and *TotC* genes were detected (* $p < 0.05$; ** $p < 0.01$, Figure 6a,b). However, downregulated relative expression levels of *Hsp70* and *Hsp26* were found in F1 females (at 600 µg/mL ZnFe₂O₄-NPs exposure, * $p < 0.05$; ** $p < 0.01$, Figure 6a), although relative expression levels of *Hsp26* was increased under 200 µg/mL exposure (** $p < 0.01$, Figure 6a). For Turandot family genes, the F1 females exhibited increased relative expressions at 200 µg/mL exposure but decreased gene expressions at 600 µg/mL (** $p < 0.01$, Figure 6b), which indicated that stress adaptation to ZnFe₂O₄-NPs exposure differed between sexes.

As shown in Figure 5, acetylcholine (ACh) and GABA levels were elevated in F1 males after ZnFe₂O₄-NPs exposure. To further elucidate the mechanism, we analyzed the expression of genes involved in neurotransmitter synthesis and circadian rhythm regulation. Males showed broad upregulations (* $p < 0.05$; ** $p < 0.01$, Figure 6c) of dopamine receptor genes (*Dα1*, *Dβ1*), choline acetyltransferase encoding gene (*ChAT*), glutamic acid decarboxylase (*Gad1*), and GABA transporter encoding gene (*Gat*). Furthermore, compared with the control groups, the exposure groups showed increased relative expressions of transcription factors involved in circadian rhythm regulation, including cycle (*Cyc*) and clock (*Clk*) genes (under 600 µg/mL dose of ZnFe₂O₄-NPs, Figure 6c). These upregulations confirm that ZnFe₂O₄-NPs exposure can induce neurotransmitter synthesis and further perturb the circadian rhythm of male flies.

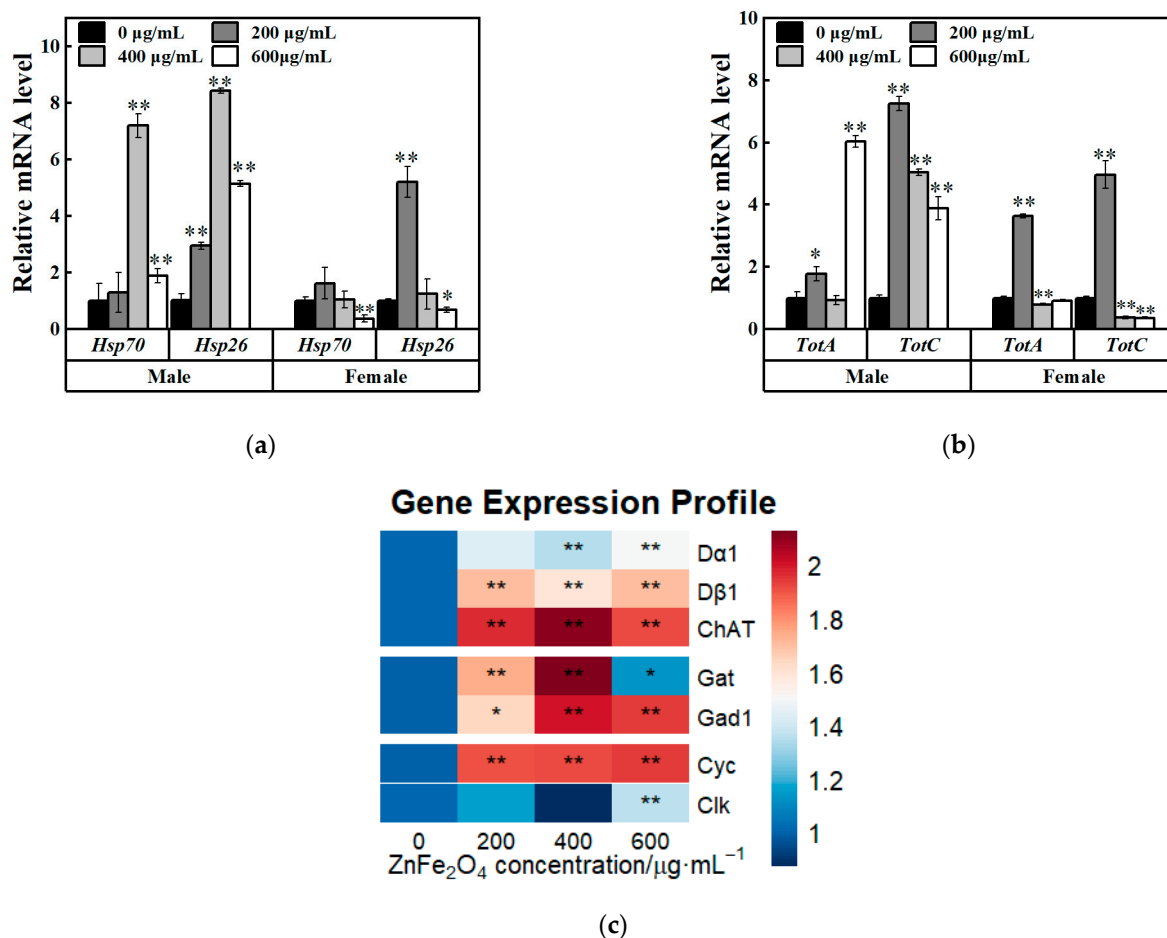


Figure 6. Expression profiles of genes in flies. (a) Changes in *Hsp26* and *Hsp70* gene expression in flies. (b) Changes in *TotA* and *TotC* gene expression in flies. (c) Changes in *Dα1*, *Dβ1*, *ChAT*, *Gat*, *Gad1*, *Cyc*, and *Clk* gene expression in flies. Values represent mean \pm SEM. (* $p < 0.05$; ** $p < 0.01$).

4. Discussion

Although ZnFe_2O_4 -NPs have garnered significant interest in biomedicine today, including applications as drug delivery vehicles and in hyperthermia-based tumor therapy, various studies have reported distinct biological interactions and context-dependent toxicity profiles [37,38]. The potential ecological risks associated with ZnFe_2O_4 -NPs exposure, particularly their effects on insect development and circadian rhythms, remain unclear. In this study, we investigated the developmental and circadian impacts of ZnFe_2O_4 -NPs exposure using *D. melanogaster* as an in vivo model.

SEM analysis revealed that average diameter of hydrothermally synthesized ZnFe_2O_4 -NPs in this study was approximately 100 nm, and TEM analysis showed that orally delivered ZnFe_2O_4 -NPs can be adhered to intestinal microvilli and internalized into gut cytoplasm of both sexes (Figure 1). Nanoscale size enabled penetration through intestinal barriers via mucus permeation and endocytosis, with microvilli as primary attachment sites [39–41]. Our results aligned with reports on other metal oxide nanoparticles in *D. melanogaster*. Our results were consistent with previous reports on metal oxide nanoparticle uptake in *D. melanogaster*. For instance, it has been demonstrated that ZnO nanoparticles can adhere to midgut microvilli in *D. melanogaster* [42]. Similarly, studies in *Xenopus laevis* have shown that ZnO nanoparticles can penetrate the gastrointestinal barrier [43]. The observed microvilli adhesion and cytoplasmic internalization of ZnFe_2O_4 -NPs mechanistically confirm intestinal barrier penetration, a critical prerequisite for the developmental and circadian disruptions documented in this study.

As shown in Figure 2, exposure to ZnFe_2O_4 -NPs can increase number of pupae and accelerate pupation progression but reduce number of eclosed adults. Increased pupal counts reflected a genuine enhancement in total progeny rather than developmental delay (Figure 2c). Developmental abnormalities occurred in response to ZnFe_2O_4 -NPs exposure. Magnetite has a highly reactive surface. It can immobilize metals and other molecules, giving it other functionalities [44]. A previous study revealed that uptake of magnetic (Fe_3O_4) nanoparticles can disturbed the oogenesis period in female *Drosophila*, which may be caused by disrupted homeostasis of trace elements such as Fe along the anterior–posterior axis of the fertilized eggs [29]. It was considered an important reason for the abnormal development of *Drosophila*. Moreover, a reduction in larval survival was identified in *Drosophila* associated with the toxic effect of dose-concentration of Chitosan-coated Fe_3O_4 -NPs, which was attributed to oxidative stress processes previously [45]. In our study, similar oxidative stress responses were confirmed by the characterization of upregulated expressions of *Hsp70* and *Hsp26*, along with inhibited T-AOC after exposure to ZnFe_2O_4 -NPs (Figures 4b and 6a). However, several reports revealed inconsistent conclusions, for instance, magnetic Fe_3O_4 can decrease reproductive capacity and reduced both pupal and adult counts [16]. This discrepancy may arise from distinct properties of different magnetic nanomaterials. Our results demonstrated that oral exposure to ZnFe_2O_4 -NPs can disrupt the developmental process of *D. melanogaster*, and this may be associated with the oxidative stress response.

Notably, we observed an increase trend of female offspring following ZnFe_2O_4 -NPs exposure (Figure 2e). This suggested that male individuals may be more susceptible to the developmental toxicity of ZnFe_2O_4 -NPs, resulting in higher mortality or developmental impairment in males. Such sex-specific sensitivity to environmental stressors has been documented in *Drosophila*; for instance, males exhibit higher mortality under thermal stress or metal exposure due to weaker antioxidant defense and higher metabolic vulnerability [46]. In addition to the abnormal development process, the male flies of F1 generation showed multiple alterations in rhythmic behaviors after intake of ZnFe_2O_4 -NPs. Activity level weakened and total sleep decreased, and exposure to high doses (400, 600/mL) led to more sleep fragmentations and more weakened unit activity capacity (Figure 3). A previous study verified that in response to reduced nutrient absorption caused by dietary changes or intestinal damage, reduced total sleep was exhibited following exposure to nano-plastics in *D. melanogaster* [47]. TEM analysis in this study revealed that flies can internalize ZnFe_2O_4 -NPs through the intestinal barrier, and elevated HSPs' gene expressions suggested that cell damage may exist in ZnFe_2O_4 -NPs-treated guts. Previous studies have manifested apoptosis after magnetite intake [48]. For instance, the guts of adult fruit flies treated with Fe_2O_4 @poly(tBGE-alt-PA) nanocomposite were identified with significant nuclear damage compared to the control group [21]. Although fragmentations of sleep were affected by ZnFe_2O_4 -NPs, we observed no significant changes on sleep and activity rhythmic patterns in *D. melanogaster* (Figure 3f,g). This result suggested that ZnFe_2O_4 -NPs may act as an adaptable environmental stressor, exerting no disruptive effects on rhythmic periodicity and showing no dose dependence within a specific range. Similarly, a previous study found that following intracerebroventricular injection, no significant disruption of circadian rhythms was observed during the maximum 1-month monitoring period post-administration across the blood–brain barrier [49].

Although ecotoxicity of ZnFe_2O_4 -NPs is poorly understood, numerous studies using different cell types or animals and different nanomaterials, have suggested that oxidative stress is a major negative effect of nanoparticle use [50,51]. Notably, our results indicated that oxidative stress responses to oral ZnFe_2O_4 -NPs differed by sex and doses (Figure 4). Males showed significant reductions, whereas females displayed enhanced activities of

SOD and CAT after ZnFe_2O_4 -NPs exposure. Notably, we found that CAT activity in male flies was an order of magnitude higher than in female flies. Similar results were found in Musachio et al.'s measurement of CAT activity in *D. melanogaster*, which indicated that the CAT activity of male flies was generally higher than that of female flies [52]. Sex-specific differences in CAT activity may act as a conserved biological feature. The results of our study showed that there was no order of magnitude difference in ROS level, which may be due to no magnitude differences between males' T-AOC and females' T-AOC (Figure 4b). T-AOC integrates the synergistic effects of multiple antioxidant components, which compensates for individual enzyme activity differences and maintains overall redox homeostasis [53]. Even if the activity of CAT enzyme changed dramatically, adjustments of the local antioxidant system and regulation of signaling molecule concentrations may still ensure the maintenance of redox homeostatic balance. In *Drosophila*, sexual differences between expressions of metallothionein have been reported under heavy metal exposures [54]. Metallothionein proteins are usually upregulated in response to diverse stimuli, including essential metals such as zinc and iron to which they specifically bind [55]. Previous reports demonstrated that ZnFe_2O_4 -NPs may not only agglomerate but also degrade and dissolve to ionic forms for their transport and storage in a non-toxic way in cells [56]. Thus, sexual differences in flies in metallothionein expression may lead to variations in the detoxification capacity of ZnFe_2O_4 -NPs. In this study, male flies exhibit lower activities of antioxidant enzymes and total antioxidant capacity (T-AOC), indicating that males are more vulnerable than females. Our findings align with recent reports demonstrating sexual dimorphism in *Drosophila*'s response to metal nanoparticle exposure, wherein males exhibit higher susceptibility [57]. Additionally compared to the control groups, both of the ROS and MDA levels exhibited significant reductions in ZnFe_2O_4 -NPs exposed groups. This found is inconsistent with prior studies, and such effects may be due to the exposed duration and special of ZnFe_2O_4 -NPs. In this study, we quantified the ROS and MDA levels of the F1 generation flies, which subjected to lifelong ZnFe_2O_4 -NPs exposure spanning embryonic to adult stages. Compared to short-term exposure, which may trigger a robust antioxidant stress response (such as increased levels of ROS and MDA [58]), long-term exposure of *Drosophila* to ZnFe_2O_4 -NPs may lead to adaptations through metabolic adaptation or active mechanisms that clear ROS and MDA. Previous studies [59,60] have confirmed that *Drosophila* can elicit ROS and MDA reduction in adaption to long-term or chronic exposure to different stress factors. Our results revealed concentration-dependent effects on MDA levels in response to ZnFe_2O_4 -NPs. MDA was significantly elevated under 400 $\mu\text{g}/\text{mL}$ exposure, while no significant difference was identified at 600 $\mu\text{g}/\text{mL}$ compared to the control, which may be caused by extensive aggregation of ZnFe_2O_4 -NPs at this concentration. As shown in Béltéky's study [61], aggregated AgNPs failed to effectively penetrate the insect intestinal cell membrane and thus led to a significant reduction in intracellular accumulation. High concentrations of AgNPs form large aggregates on the surface of intestinal villi and inside cells, which may further correlate with a decline in MDA levels [62].

Moreover, significant increase in expression levels of heat shock protein genes (Figure 6a, *Hsp26*, *Hsp70*) and Turandot protein genes (Figure 6b, *TotA*, *TotC*) in both sexes were identified in this study, which further suggested that oxidative stress responses were induced by ZnFe_2O_4 -NPs. In *D. melanogaster*, silver nanoparticles can activate heat shock protein 70, oxidative stress and apoptosis [63]. Oxidative stress induced by silica nanoparticles might have been involved in proinflammatory responses [64]. Turandot genes, like HSPs, have been characterized to respond to a variety of stress types such as heat stress, cold stress, irradiation, infection, dehydration, oxidative agents, and mechanical stress [65]. Thus, flies may activate Turandot genes expressions in respond to ZnFe_2O_4 -NPs exposure that can be considered as an adaptable stress factor. In our study, we observed

a distinct concentration-dependent pattern for HSPs. High nanoparticle concentration exposure may inhibit HSPs' production. Upregulated expression levels of HSPs were detected at 400 µg/mL in male flies and 200 µg/mL in female flies, while expression levels were declined significantly under 600 µg/mL exposure (Figure 6a). This decline may be attributed to the aggregation of ZnFe₂O₄-NPs, which can reduce the cellular bioavailability of the nanoparticles. Similar results were founded that high concentrations of AgNPs tend to aggregate and decreased the uptake efficiency in insect gut cells [61]. For ZnFe₂O₄-NPs, aggregation may occur at 600 µg/mL concentration and can induce reduction in bioavailability, ultimately leading to lower heat shock protein production. TotA's mRNA levels in females also indicated that aggregated ZnFe₂O₄-NPs nanoparticles may occur under high concentrations. A concentration of 200 µg/mL is the maximum for female flies, and high concentrations reduced the production compared to the maximum, even inhibit it compared to the control. However, the expression level of TotA in male flies under 600 µg/mL was highly upregulated, which was different with the females' pattern. This may due to sex-specific differences in *Drosophila* in response to different stressors [66].

This study investigated the impact of ZnFe₂O₄-NPs on *Drosophila* activity and sleep, revealing significant effects: weakened activity capacity, shortened total sleep time and increased sleep fragmentations (Figure 3). These findings align with previous research demonstrating that exposure to strontium ferrite and magnetic iron oxide nanoparticles similarly reduces climbing ability in fruit flies [67]. Simultaneously, ZnFe₂O₄-NPs treatment increased the expression of core clock genes *Cyc* or *Clk* in *Drosophila* (Figure 6), potentially disturbing circadian neurons governing sleep–wake transitions and contributing to unstable sleep and frequent awakenings [68,69]. Altered reactive oxygen species (ROS) levels, which has been confirmed as a consequence of ZnFe₂O₄-NPs exposure, can disrupt the circadian clock, which functions to minimize oxidative damage by regulating rhythmic processes [70]. Concurrently, we found elevated levels of the neurotransmitters ACh and GABA in *Drosophila* (Figure 5), and gene expression analysis revealed upregulations of dopamine receptors genes (*Dα1*, *Dβ1*), Choline acetyltransferase (*ChAT*), Glutamic acid decarboxylase (*Gad1*), and GABA transporter (*Gat*) (Figure 6). These findings indicated the enhanced synthesis of neurotransmitters. Elevated ACh levels promote wakefulness [71,72], which can increase sleep fragmentation and reduce stability [73], correlating with the observed increased sleep episodes of flies [74]. GABA is primarily an inhibitory neurotransmitter promoting sleep [75], its increased levels, potentially exacerbated by nanomaterial exposure, may excessively suppress neuronal activity and reduce locomotion [76]. Critically, ZnFe₂O₄-NPs directly drive neurotransmitter alterations through transcriptional activation. Notably, GABA functions dually as both a neurotransmitter and an endogenous antioxidant, and its increase likely contributes to ROS suppression. Therefore, ZnFe₂O₄-NPs likely can impair sleep quality and activity capacity in *Drosophila* through combined disruptions of the circadian clock and dysregulation of neurotransmitter systems.

5. Conclusions

In this study, the effects of ZnFe₂O₄-NPs on *D. melanogaster* were investigated. The results indicated that ZnFe₂O₄-NPs can enter the gut tissue and act as an external stimulus to upregulate the gene expression levels of HSPs and Turandot proteins, leading to alterations in numbers of pupae and eclosed adults and abnormality of development process. Concurrently, exposure to ZnFe₂O₄-NPs can affect the rhythmic behaviors of *D. melanogaster*, leading to weakened activity capacity, significant reduction in total sleep time and increased sleep fragmentations in males. Such effects may be due to the induced oxidative stress responses, increased neurotransmitter levels and upregulated expression levels of circadian genes via exposure of ZnFe₂O₄-NPs. Our study further elucidated

the response of insect like organisms to ZnFe_2O_4 -NPs, providing a basis for the rational evaluation of the ecological safety of ZnFe_2O_4 -NPs. Our findings may provide insights for evaluating ecological risks of metal-based NPs and suggest applications in developing pest management strategies via insect responses to nanomaterials.

Supplementary Materials: The following supporting information can be downloaded at: <https://www.mdpi.com/article/10.3390/toxics13090779/s1>. The primer sequences mentioned in this study were supplied in Supplementary Table S1.

Author Contributions: Conceptualization, W.Y. and Y.S.; methodology, W.Y., Y.S. and P.L.; software, Y.G.; formal analysis, Z.Z. and J.Y.; investigation, W.Y.; data curation, W.Y.; writing—original draft preparation, W.Y. and Y.S.; supervision, Y.S. and J.Y.; project administration, Y.S. All authors have read and agreed to the published version of the manuscript.

Funding: This research was funded by National Natural Science Foundation of China, grant number 32201017; and Tianjin Key Research and Development Program, grant number 22YFYZH00280.

Institutional Review Board Statement: Not applicable.

Informed Consent Statement: Not applicable.

Data Availability Statement: The original contributions presented in this study are included in the article. Further inquiries can be directed to the corresponding author.

Acknowledgments: The authors would like to thank the *Drosophila* Resource and Technology Platform of the Institute of Biochemistry and Cell Biology, Shanghai Institutes for Biological Sciences, Chinese Academy of Sciences, for providing the *Drosophila* strains essential to this study.

Conflicts of Interest: The authors declare no conflicts of interest.

References

1. Ibrahim, A.A.; Saed, M.; Al Abdullah, S.; Dellinger, K.; Obare, S.O.; Pathiraja, G. Magnetic zinc ferrite nanostructures: Recent advancements for environmental and biomedical applications. *J. Alloys Compd.* **2024**, *4*, 100038. [\[CrossRef\]](#)
2. Zimina, T.M.; Sitkov, N.O.; Gareev, K.G.; Fedorov, V.; Grouzdev, D.; Koziaeva, V.; Gao, H.; Combs, S.E.; Shevtsov, M. Biosensors and Drug Delivery in Oncotheranostics Using Inorganic Synthetic and Biogenic Magnetic Nanoparticles. *Biosensors* **2022**, *12*, 789. [\[CrossRef\]](#)
3. Rezaei, B.; Yari, P.; Sanders, S.M.; Wang, H.; Chugh, V.K.; Liang, S.; Mostufa, S.; Xu, K.; Wang, J.P.; Gómez-Pastora, J.; et al. Magnetic Nanoparticles: A Review on Synthesis, Characterization, Functionalization, and Biomedical Applications. *Small* **2024**, *20*, e2304848. [\[CrossRef\]](#)
4. Liu, W.; Dong, Z.; Liu, J.; Li, Z.; Wang, Y.; Cao, X.; Zhang, Z.; Liu, Y. Hollow S-Doped ZnFe_2O_4 Microcubes with Magnetic Separability for Photocatalytic Removal of Uranium(VI) under Different Light Intensity. *Inorg. Chem.* **2024**, *63*, 11369–11380. [\[CrossRef\]](#)
5. Omelyanchik, A.; Levada, K.; Pshenichnikov, S.; Abdolrahim, M.; Baricic, M.; Kapitunova, A.; Galieva, A.; Sukhikh, S.; Astakhova, L.; Antipov, S.; et al. Green Synthesis of Co-Zn Spinel Ferrite Nanoparticles: Magnetic and Intrinsic Antimicrobial Properties. *Materials* **2020**, *13*, 5014. [\[CrossRef\]](#)
6. Rabbani, A.; Haghniaz, R.; Khan, T.; Khan, R.; Khalid, A.; Naz, S.S.; Ul-Islam, M.; Vajhadin, F.; Wahid, F. Development of bactericidal spinel ferrite nanoparticles with effective biocompatibility for potential wound healing applications. *RSC Adv.* **2021**, *11*, 1773–1782. [\[CrossRef\]](#)
7. Qin, H.; He, Y.; Xu, P.; Huang, D.; Wang, Z.; Wang, H.; Wang, Z.; Zhao, Y.; Tian, Q.; Wang, C. Spinel ferrites (MFe_2O_4): Synthesis, improvement and catalytic application in environment and energy field. *Adv. Colloid Interface Sci.* **2021**, *294*, 102486. [\[CrossRef\]](#) [\[PubMed\]](#)
8. Tabesh, F.; Mallakpour, S.; Hussain, C.M. Recent advances in magnetic semiconductor ZnFe_2O_4 nanoceramics: History, properties, synthesis, characterization, and applications. *J. Solid State Chem.* **2023**, *322*, 123940. [\[CrossRef\]](#)
9. Ferrite Market—Forecast (2025–2031). Available online: <https://www.industryarc.com/Report/15854/ferrite-market.html> (accessed on 14 August 2025).
10. Nowack, B. Evaluation of Environmental Exposure Models for Engineered Nanomaterials in a Regulatory Context. *NanoImpact* **2017**, *8*, 38–47. [\[CrossRef\]](#)

11. Thakur, D.; Ta, Q.T.H.; Noh, J.S. Photosensitizer-Conjugated Hollow ZnFe₂O₄ Nanoparticles for Antibacterial Near-Infrared Photodynamic Therapy. *ACS Appl. Nano Mater.* **2022**, *5*, 1533–1541. [\[CrossRef\]](#)
12. Nguyen, V.V.H.; Chu, M.H.; Nguyen, D.H.; Nguyen, V.D.; Park, I.; Nguyen, V.H. Excellent detection of H₂S gas at ppb concentrations using ZnFe₂O₄ nanofibers loaded with reduced graphene oxide. *Sens. Actuators B Chem.* **2019**, *282*, 876–884. [\[CrossRef\]](#)
13. Xu, Z.; Long, X.; Jia, Y.; Zhao, D.; Pan, X. Occurrence, transport, and toxicity of nanomaterials in soil ecosystems: A review. *Environ. Chem. Lett.* **2022**, *20*, 3943–3969. [\[CrossRef\]](#)
14. Tao, Z.; Zhou, Q.; Zheng, T.; Mo, F.; Ouyang, S. Iron oxide nanoparticles in the soil environment: Adsorption, transformation, and environmental risk. *J. Hazard. Mater.* **2023**, *459*, 132107. [\[CrossRef\]](#)
15. Surendra, D.M.; Chamaraja, N.A.; Godipurge, S.S.; Yallappa, S. Synthesis and functionalization of silver ferrite (AgFe₂O₃) nanoparticles with l-methionine: In vivo toxicity studies against *Drosophila melanogaster* (Diptera: Drosophilidae). *Results Chem.* **2022**, *4*, 100565. [\[CrossRef\]](#)
16. Pilaquinga, F.; Cárdenas, S.; Vela, D.; Jara, E.; Morey, J.; Gutiérrez-Coronado, J.L.; Debut, A.; Piña, M.L.N. Fertility and Iron Bioaccumulation in *Drosophila melanogaster* Fed with Magnetite Nanoparticles Using a Validated Method. *Molecules* **2021**, *26*, 2808. [\[CrossRef\]](#) [\[PubMed\]](#)
17. Güneş, M.; Aktaş, K.; Yalçın, B.; Burgazlı, A.Y.; Asilturk, M.; Ünşar, A.E.; Kaya, B. In vivo assessment of the toxic impact of exposure to magnetic iron oxide nanoparticles (IONPs) using *Drosophila melanogaster*. *Environ Toxicol. Pharmacol.* **2024**, *107*, 104412. [\[CrossRef\]](#) [\[PubMed\]](#)
18. Bag, J.; Mukherjee, S.; Ghosh, S.K.; Das, A.; Mukherjee, A.; Sahoo, J.K.; Tung, K.S.; Sahoo, H.; Mishra, M. Fe₃O₄ coated guar gum nanoparticles as non-genotoxic materials for biological application. *Int. J. Biol. Macromol.* **2020**, *165*, 333–345. [\[CrossRef\]](#)
19. Malhotra, N.; Chen, J.R.; Sarasamma, S.; Audira, G.; Siregar, P.; Liang, S.T.; Lai, Y.H.; Lin, G.M.; Ger, T.R.; Hsiao, C.D. Ecotoxicity Assessment of Fe₃O₄ Magnetic Nanoparticle Exposure in Adult Zebrafish at an Environmental Pertinent Concentration by Behavioral and Biochemical Testing. *Nanomaterials* **2019**, *9*, 873. [\[CrossRef\]](#)
20. Tawfik, M.M.; Mohamed, M.H.; Sadak, M.S.; Thalooth, A.T. Iron oxide nanoparticles effect on growth, physiological traits and nutritional contents of *Moringa oleifera* grown in saline environment. *Bull. Natl. Res. Cent.* **2021**, *45*, 177. [\[CrossRef\]](#)
21. Chauhan, S.; Naik, S.; Kumar, R.; Ruokolainen, J.; Kesari, K.K.; Mishra, M.; Gupta, P.K. In Vivo Toxicological Analysis of the ZnFe₂O₄@poly(tBGE-alt-PA) Nanocomposite: A Study on Fruit Fly. *ACS Omega* **2024**, *9*, 6549–6555. [\[CrossRef\]](#)
22. Ong, C.; Yung, L.Y.; Cai, Y.; Bay, B.H.; Baeg, G.H. *Drosophila melanogaster* as a model organism to study nanotoxicity. *Nanotoxicology* **2015**, *9*, 396–403. [\[CrossRef\]](#)
23. Parashar, S.; Raj, S.; Srivastava, P.; Singh, A.K. Comparative toxicity assessment of selected nanoparticles using different experimental model organisms. *J. Pharmacol. Toxicol. Methods* **2024**, *130*, 107563. [\[CrossRef\]](#)
24. Ng, C.T.; Yu, L.E.; Ong, C.N.; Bay, B.H.; Baeg, G.H. The use of *Drosophila melanogaster* as a model organism to study immune-nanotoxicity. *Nanotoxicology* **2019**, *13*, 429–446. [\[CrossRef\]](#)
25. Raj, A.; Shah, P.; Agrawal, N. Sedentary behavior and altered metabolic activity by AgNPs ingestion in *Drosophila melanogaster*. *Sci. Rep.* **2017**, *7*, 15617. [\[CrossRef\]](#)
26. Gautam, A.; Gautam, C.; Mishra, M.; Mishra, V.K.; Hussain, A.; Sahu, S.; Nanda, R.; Kisan, B.; Biradar, S.; Gautam, R.K. Enhanced mechanical properties of hBN-ZrO₂ composites and their biological activities on *Drosophila melanogaster*: Synthesis and characterization. *RSC Adv.* **2019**, *9*, 40977–40996. [\[CrossRef\]](#)
27. Parmalee, N.L.; Aschner, M. Metals and Circadian Rhythms. *Adv. Neurotoxicol.* **2017**, *1*, 119–130. [\[CrossRef\]](#) [\[PubMed\]](#)
28. Sullivan, W.; Ashburner, M.; Hawley, R.S. *Drosophila Protocols*; Science Press: Beijing, China, 2004; pp. 589–590.
29. Chen, H.; Wang, B.; Feng, W.; Du, W.; Ouyang, H.; Chai, Z.; Bi, X. Oral magnetite nanoparticles disturb the development of *Drosophila melanogaster* from oogenesis to adult emergence. *Nanotoxicology* **2015**, *9*, 302–312. [\[CrossRef\]](#) [\[PubMed\]](#)
30. Wang, Y.X. Superparamagnetic iron oxide based MRI contrast agents: Current status of clinical application. *Quant. Imaging Med. Surg.* **2011**, *1*, 35–40. [\[CrossRef\]](#) [\[PubMed\]](#)
31. Rocabert, A.; Martín-Pérez, J.; Pareras, L.; Egea, R.; Alaraby, M.; Cabrera-Gumbau, J.M.; Sarmiento, I.; Martínez-Urtaza, J.; Rubio, L.; Bargailla, I.; et al. Nanoplastic exposure affects the intestinal microbiota of adult *Drosophila* flies. *Sci. Total Environ.* **2025**, *980*, 179545. [\[CrossRef\]](#)
32. Wang, Y.; Zhang, H.; Zhang, Z.; Sun, B.; Tang, C.; Zhang, L.; Jiang, Z.; Ding, B.; Liao, Y.; Cai, P. Simulated mobile communication frequencies (3.5 GHz) emitted by a signal generator affects the sleep of *Drosophila melanogaster*. *Environ. Pollut.* **2021**, *283*, 117087. [\[CrossRef\]](#)
33. Donelson, N.C.; Kim, E.Z.; Slawson, J.B.; Vecsey, C.G.; Huber, R.; Griffith, L.C. High-resolution positional tracking for long-term analysis of *Drosophila* sleep and locomotion using the “tracker” program. *PLoS ONE* **2012**, *7*, e37250. [\[CrossRef\]](#)
34. Livak, K.J.; Schmittgen, T.D. Analysis of Relative Gene Expression Data Using Real-Time Quantitative PCR and the 2^{−ΔΔCT} Method. *Methods* **2001**, *25*, 402–408. [\[CrossRef\]](#)

35. Rommelaere, S.; Carboni, A.; Bada Juarez, J.F.; Boquete, J.P.; Abriata, L.A.; Teixeira Pinto Meireles, F.; Rukes, V.; Vincent, C.; Kondo, S.; Dionne, M.S.; et al. A humoral stress response protects *Drosophila* tissues from antimicrobial peptides. *Curr. Biol.* **2024**, *34*, 1426–1437.e6. [\[CrossRef\]](#)
36. Amstrup, A.B.; Bæk, I.; Loeschcke, V.; Givskov Sørensen, J. A functional study of the role of Turandot genes in *Drosophila melanogaster*: An emerging candidate mechanism for inducible heat tolerance. *J. Insect Physiol.* **2022**, *143*, 104456. [\[CrossRef\]](#)
37. Bushra, R.; Ahmad, M.; Alam, K.; Seidi, F.; Qurtulen; Shakeel, S.; Song, J.; Jin, Y.; Xiao, H. Recent advances in magnetic nanoparticles: Key applications, environmental insights, and future strategies. *Sustain. Mater. Technol.* **2024**, *40*, e00985. [\[CrossRef\]](#)
38. Soares, G.A.; Faria, J.V.C.; Pinto, L.A.; Prospero, A.G.; Pereira, G.M.; Stoppa, E.G.; Buranello, L.P.; Bakuzis, A.F.; Baffa, O.; Miranda, J.R.A. Long-Term Clearance and Biodistribution of Magnetic Nanoparticles Assessed by AC Biosusceptometry. *Materials* **2022**, *15*, 2121. [\[CrossRef\]](#) [\[PubMed\]](#)
39. Xu, M.; Qi, Y.; Liu, G.; Song, Y.; Jiang, X.; Du, B. Size-Dependent In Vivo Transport of Nanoparticles: Implications for Delivery, Targeting, and Clearance. *ACS Nano* **2023**, *17*, 20825–20849. [\[CrossRef\]](#) [\[PubMed\]](#)
40. Saeedi, M.; Eslamifar, M.; Khezri, K.; Dizaj, S.M. Applications of nanotechnology in drug delivery to the central nervous system. *Biomed. Pharmacother.* **2019**, *111*, 666–675. [\[CrossRef\]](#)
41. Manzanares, D.; Ceña, V. Endocytosis: The Nanoparticle and Submicron Nanocompounds Gateway into the Cell. *Pharmaceutics* **2020**, *12*, 371. [\[CrossRef\]](#)
42. Alaraby, M.; Annangi, B.; Hernández, A.; Creus, A.; Marcos, R. A comprehensive study of the harmful effects of ZnO nanoparticles using *Drosophila melanogaster* as an in vivo model. *J. Hazard. Mater.* **2015**, *296*, 166–174. [\[CrossRef\]](#)
43. Bacchetta, R.; Moschini, E.; Santo, N.; Fascio, U.; Del Giacco, L.; Freddi, S.; Camatini, M.; Mantecca, P. Evidence and uptake routes for Zinc oxide nanoparticles through the gastrointestinal barrier in *Xenopus laevis*. *Nanotoxicology* **2013**, *8*, 728–744. [\[CrossRef\]](#) [\[PubMed\]](#)
44. Iacovita, C.; Stiuflu, R.; Radu, T.; Florea, A.; Stiuflu, G.; Dutu, A.; Mican, S.; Tetea, R.; Lucaciu, C.M. Polyethylene Glycol-Mediated Synthesis of Cubic Iron Oxide Nanoparticles with High Heating Power. *Nanoscale Res. Lett.* **2015**, *10*, 391. [\[CrossRef\]](#)
45. Vela, D.; Rondal, J.; Cárdenas, S.; Gutiérrez-Coronado, J.; Jara, E.; Debut, A.; Pilaquinga, F. Assessment of the Toxic Effects of Chitosan-Coated Magnetite Nanoparticles on *Drosophila melanogaster*. *Am. J. Appl. Sci.* **2020**, *17*, 204–213. [\[CrossRef\]](#)
46. Faria, F.S.; Areal, M.; Bitner-Mathé, B.C. Thermal Stress and Adult Fitness in a *Drosophila suzukii* Neotropical Propagule. *Neotrop. Entomol.* **2023**, *52*, 993–1004. [\[CrossRef\]](#)
47. Matthews, S.; Xu, E.G.; Roubeau Dumont, E.; Meola, V.; Pikuda, O.; Cheong, R.; Guo, M.; Tahara, R.; Larsson, H.; Tufenkji, N. Polystyrene micro- and nanoplastics affect locomotion and daily activity of *Drosophila melanogaster*. *Environ. Sci. Nano* **2021**, *8*, 110–121. [\[CrossRef\]](#)
48. Adamczyk-Grochala, J.; Wnuk, M.; Oklejewicz, B.; Klimczak, K.; Błoniarz, D.; Deręgowska, A.; Rzeszutek, I.; Stec, P.; Ciurazkiewicz, A.; Kadziółka-Gawęł, M.; et al. Evaluation of anticancer activity of urotropine surface modified iron oxide nanoparticles using a panel of forty breast cancer cell lines. *Nanotoxicology* **2025**, *19*, 50–68. [\[CrossRef\]](#)
49. Zhang, P.; Zhou, L.; Xu, H.F.; Dai, Z.H.; Hao, W.; Cao, J.M. Effect of Fe₂O₃ Magnetic Nanoparticles on Circadian Rhythm in Mice. In *Proceedings of the 23rd National Congress of the Chinese Association for Physiological Sciences, Xi'an, China, 18–21 October 2010*; Department of Physiology and Pathophysiology, Institute of Basic Medical Sciences, Chinese Academy of Medical Sciences & Peking Union Medical College, Eds.; Science Press: Beijing, China, 2010; pp. 230–231.
50. Ma, P.; Luo, Q.; Chen, J.; Gan, Y.; Du, J.; Ding, S.; Xi, Z.; Yang, X. Intraperitoneal injection of magnetic Fe₃O₄-nanoparticle induces hepatic and renal tissue injury via oxidative stress in mice. *Int. J. Nanomed.* **2012**, *7*, 4809–4818. [\[CrossRef\]](#)
51. Yu, S.; Rui, Q.; Cai, T.; Wu, Q.; Li, Y.; Wang, D. Close association of intestinal autofluorescence with the formation of severe oxidative damage in intestine of nematodes chronically exposed to Al₂O₃-nanoparticle. *Environ. Toxicol. Pharmacol.* **2011**, *32*, 233–241. [\[CrossRef\]](#)
52. Musachio, E.A.S.; Poetini, M.R.; Janner, D.E.; Meichtry, L.B.; Poleto, K.H.; Fernandes, E.J.; Guerra, G.P.; Prigol, M. Sex-specific changes in oxidative stress parameters and longevity produced by Bisphenol F and S compared to Bisphenol A in *Drosophila melanogaster*. *Comp. Biochem. Physiol. Part C Toxicol. Pharmacol.* **2022**, *257*, 109329. [\[CrossRef\]](#) [\[PubMed\]](#)
53. Sies, H.; Jones, D.P. Reactive oxygen species (ROS) as pleiotropic physiological signalling agents. *Nat. Rev. Mol. Cell Biol.* **2020**, *21*, 363–383. [\[CrossRef\]](#) [\[PubMed\]](#)
54. Slobodian, M.R.; Petahtegoose, J.D.; Wallis, A.L.; Levesque, D.C.; Merritt, T.J.S. The Effects of Essential and Non-Essential Metal Toxicity in the *Drosophila melanogaster* Insect Model: A Review. *Toxics* **2021**, *9*, 269. [\[CrossRef\]](#)
55. Qiang, W.; Huang, Y.; Wan, Z.; Zhou, B. Metal-metal interaction mediates the iron induction of *Drosophila* MtnB. *Biochem. Biophys. Res. Commun.* **2017**, *487*, 646–652. [\[CrossRef\]](#) [\[PubMed\]](#)
56. Rivero, M.; Marín-Barba, M.; Gutiérrez, L.; Lozano-Velasco, E.; Wheeler, G.N.; Sánchez-Marcos, J.; Muñoz-Bonilla, A.; Morris, C.J.; Ruiz, A. Toxicity and biodegradation of zinc ferrite nanoparticles in *Xenopus laevis*. *J. Nanopart. Res.* **2019**, *21*, 181. [\[CrossRef\]](#)
57. Alaraby, M.; Abass, D.; Gutiérrez, J.; Velázquez, A.; Hernández, A.; Marcos, R. Reproductive Toxicity of Nanomaterials Using Silver Nanoparticles and *Drosophila* as Models. *Molecules* **2024**, *29*, 5802. [\[CrossRef\]](#)

58. Yang, P.; Yang, X.; Sun, L.; Han, X.; Xu, L.; Gu, W.; Zhang, M. Effects of cadmium on oxidative stress and cell apoptosis in *Drosophila melanogaster* larvae. *Sci. Rep.* **2022**, *12*, 4762. [[CrossRef](#)]
59. Pickering, A.M.; Vojtovich, L.; Tower, J.; Davies, K.J.A. Oxidative stress adaptation with acute, chronic, and repeated stress. *Free Radic. Biol. Med.* **2013**, *55*, 109–118. [[CrossRef](#)]
60. Medina-Leendertz, S.; Mora, M.; Vielma, J.R.; Bravo, Y.; Atencio-Bracho, L.; Leal-Yépez, A.; Arcaya, J.L.; Bonilla, E. Melatonin decreases oxidative stress in *Drosophila melanogaster* exposed to manganese. *Investig. Clin.* **2018**, *59*, 230–241. [[CrossRef](#)]
61. Béltéky, P.; Rónavári, A.; Igaz, N.; Szerencsés, B.; Tóth, I.Y.; Pfeiffer, I.; Kiricsi, M.; Kónya, Z. Silver nanoparticles: Aggregation behavior in biorelevant conditions and its impact on biological activity. *Int. J. Nanomed.* **2019**, *14*, 667–687. [[CrossRef](#)] [[PubMed](#)]
62. Wang, Z.; Zhang, L.; Wang, X. Molecular toxicity and defense mechanisms induced by silver nanoparticles in *Drosophila melanogaster*. *J. Environ. Sci.* **2023**, *125*, 616–629. [[CrossRef](#)]
63. Ahamed, M.; Posgai, R.; Gorey, T.J.; Nielsen, M.; Hussain, S.M.; Rowe, J.J. Silver nanoparticles induced heat shock protein 70, oxidative stress and apoptosis in *Drosophila melanogaster*. *Toxicol. Appl. Pharmacol.* **2010**, *242*, 263–269. [[CrossRef](#)]
64. Park, E.J.; Park, K. Oxidative stress and pro-inflammatory responses induced by silica nanoparticles in vivo and in vitro. *Toxicol. Lett.* **2009**, *184*, 18–25. [[CrossRef](#)]
65. Ekengren, S.; Hultmark, D. A family of Turandot-related genes in the humoral stress response of *Drosophila*. *Biochem. Biophys. Res. Commun.* **2001**, *284*, 998–1003. [[CrossRef](#)] [[PubMed](#)]
66. Mukherjee, S.; Nayak, N.; Mohapatra, S.; Sahoo, J.K.; Sahoo, H.; Mishra, M. Strontium ferrite as a nontoxic nanomaterial to improve metabolism in a diabetic model of *Drosophila melanogaster*. *Mater. Chem. Phys.* **2022**, *281*, 125906. [[CrossRef](#)]
67. Ekengren, S.; Tryselius, Y.; Dushay, M.S.; Liu, G.; Steiner, H.; Hultmark, D. A humoral stress response in *Drosophila*. *Curr. Biol.* **2001**, *11*, 1479. [[CrossRef](#)]
68. Tataroglu, O.; Emery, P. Studying circadian rhythms in *Drosophila melanogaster*. *Methods* **2014**, *68*, 140–150. [[CrossRef](#)]
69. Parasram, K.; Bachetti, D.; Carmona-Alcocer, V.; Karpowicz, P. Fluorescent Reporters for Studying Circadian Rhythms in *Drosophila melanogaster*. *Methods Mol. Biol.* **2022**, *2482*, 353–371. [[CrossRef](#)]
70. Masuda, K.; Sakurai, T.; Hirano, A. A coupled model between circadian, cell-cycle, and redox rhythms reveals their regulation of oxidative stress. *Sci. Rep.* **2024**, *14*, 15479. [[CrossRef](#)]
71. Xiao, N.; Xu, S.; Li, Z.K.; Tang, M.; Mao, R.; Yang, T.; Ma, S.X.; Wang, P.H.; Li, M.T.; Sunilkumar, A.; et al. A single photoreceptor splits perception and entrainment by cotransmission. *Nature* **2023**, *623*, 562–570. [[CrossRef](#)] [[PubMed](#)]
72. Roach, J.P.; Ben-Jacob, E.; Sander, L.M.; Zochowski, M.R. Modeling the formation and dynamics of cortical waves induced by cholinergic modulation. *BMC Neurosci.* **2015**, *16* (Suppl. 1), P304. [[CrossRef](#)]
73. Jones, B.E. Arousal and sleep circuits. *Neuropsychopharmacology* **2020**, *45*, 6–20. [[CrossRef](#)]
74. Tang, J.; Liu, A.; Chen, K.; Shi, Y.; Qiu, X. Exposure to amitriptyline disturbs behaviors in adult zebrafish and their offspring via altering neurotransmitter levels. *Comp. Biochem. Physiol. C Toxicol. Pharmacol.* **2025**, *288*, 110079. [[CrossRef](#)] [[PubMed](#)]
75. Chaturvedi, R.; Emery, P. Fly into tranquility: GABA's role in *Drosophila* sleep. *Curr. Opin. Insect Sci.* **2024**, *64*, 101219. [[CrossRef](#)] [[PubMed](#)]
76. Ossowska, K. Zona incerta as a therapeutic target in Parkinson's disease. *J. Neurol.* **2020**, *267*, 591–606. [[CrossRef](#)] [[PubMed](#)]

Disclaimer/Publisher's Note: The statements, opinions and data contained in all publications are solely those of the individual author(s) and contributor(s) and not of MDPI and/or the editor(s). MDPI and/or the editor(s) disclaim responsibility for any injury to people or property resulting from any ideas, methods, instructions or products referred to in the content.